Purification and Characterization of Smooth Muscle Cell Caveolae

Wen-Jinn Chang,* Yun-shu Ying,* Karen G. Rothberg,* Nigel M. Hooper,§ Anthony J. Turner,§ Hervé A. Gambliel,* Jean De Gunzburg,‖ Susanne M. Mumby,‡ Alfred G. Gilman,‡ and Richard G. W. Anderson*

*Departments of Cell Biology and Neuroscience, and ‡Pharmacology, University of Texas Southwestern Medical Center at Dallas, Dallas, Texas 75235; §Department of Biochemistry and Molecular Biology, University of Leeds, Leeds LS2 9JT, United Kingdom; and ‖Institut National de la Santé et de La Recherche Médicale, Unité 248, Faculté de Medecine Lariboisière-Saint Louis, Paris, France

Abstract. Plasmalemmal caveolae are a membrane specialization that mediates transcytosis across endothelial cells and the uptake of small molecules and ions by both epithelial and connective tissue cells. Recent findings suggest that caveolae may, in addition, be involved in signal transduction. To better understand the molecular composition of this membrane specialization, we have developed a biochemical method for purifying caveolae from chicken smooth muscle cells. Biochemical and morphological markers indicate that we can obtain ~1.5 mg of protein in the caveolae fraction from ~100 g of chicken gizzard. Gel electrophoresis shows that there are more than 30 proteins enriched in caveolae relative to the plasma membrane. Among these proteins are: caveolin, a structural molecule of the caveolae coat; multiple, glycosylphosphatidylinositol-anchored membrane proteins; both G_α and G_β subunits of heterotrimeric GTP-binding protein; and the Ras-related GTP-binding protein, Rap1A/B. The method we have developed will facilitate future studies on the structure and function of caveolae.

THERE is increasing evidence that plasmalemmal caveolae are a membrane specialization capable of sealing off from the extracellular environment to create a unique, membrane bound compartment at the cell surface. The dynamics of caveolae opening and closing is best observed in endothelial cells (46, 47), where they appear to form plasmalemmal vesicles that move across the cell and fuse with the abluminal membrane. Each round of caveolae-mediated transcytosis transports a portion of molecules from the blood to the tissue space without merging with other endocytic pathways. Although in other cell types the budding event has not been seen with the electron microscope, biochemical studies have shown (17–19) that caveolae can sequester membrane bound ligands away from the extracellular space and facilitate their delivery to the cytoplasm of the cell. This process is called potocytosis (3).

What distinguishes potocytosis from other endocytic pathways is the use of glycosylphosphatidylinositol (GPI)[1]-anchored membrane proteins to concentrate low molecular weight molecules and ions in closed caveolae (22, 41). Morphological (54) and biochemical (5, 7) methods have documented that a variety of different cell types contain highly clustered arrays of GPI-anchored membrane proteins and that a subset of these clusters is in caveolae (43, 54). The cytoplasmic surface of each caveolae has a characteristic striated coat that is composed of integral membrane proteins (35, 39). The integrity of this coat (39), as well as the clustering of the GPI-anchored proteins (6, 40), is dependent on the presence of cholesterol in the membrane. Therefore, the structure of caveolae is highly dependent on the lipid composition of the membrane.

Potocytosis may be a mechanism for delivering signaling molecules or ions to the cell (2, 3). An extension of this idea is that caveolae can sometimes store or process incoming and outgoing cellular messengers (1). These proposals are based on the finding that certain of the molecules associated with caveolae are known to participate either directly or indirectly in cell signaling. One example is caveolin, an integral membrane component of the caveolar coat (39). The phosphorylation of this protein by $pp60^{v\text{-}src}$ is tightly coupled to the transformation of chick embryo fibroblasts by the Rous sarcoma virus (13). This suggests that abnormal cell–cell and cell–substratum interactions, which result in the transformed phenotype, may be the consequence of caveolin being phosphorylated on tyrosine. GPI-anchored membrane proteins themselves have been implicated as the source of inositolphosphoglycans (IPG) that act as second messengers for a variety of different hormones (37, 38, 42). In addition, 1,4,5-triphosphate (IP3) sensitive calcium channels (12), as well

Address all correspondence to Dr. Richard G. W. Anderson, Department of Cell Biology and Neuroscience, University of Texas Southwestern Medical Center, Dallas, TX 75235.

1. *Abbreviations used in this paper*: CRD, cross-reacting determinant; GPI, glycosylphosphatidylinositol; IPG, inositolphosphoglycans; IP3, 1,4,5-trisphosphate; PI-PLC, phosphatidylinositol specific phospholipase C.

as an ATP-dependent calcium pump (11), have been recently localized to caveolae, which suggests a role for potocytosis in calcium signaling. Finally, non-receptor tyrosine kinases have been found associated with isolated GPI anchor clusters (48, 50) and caveolin-rich membrane fractions (43). These kinases are activated by the binding of antibodies to GPI-anchored proteins (44).

The eventual understanding of how caveolae function in the cell will depend on the development of purification schemes that allow investigators to obtain large quantities of this organelle for biochemical analysis. Recently, Sargiacomo et al. (43) described an analytical method for obtaining caveolin-rich membrane fractions from cultured fibroblasts. We now report on the development of a method for purifying biochemical quantities of caveolae from chicken gizzard smooth muscle cells. In addition to being enriched in at least 30 different proteins, these caveolae appear to be a cell surface location for small and heterotrimeric GTP-binding proteins.

Materials and Methods

Materials

Triton X-100, β-mercaptoethanol, glycerin, crystalline BSA, leupeptin, sodium chloride, sodium azide, potassium iodide, sucrose, fish gelatin, EDTA, EGTA, MOPS, NP-40, soybean trypsin inhibitor, pepstatin A, N-ethylmaleimide, and benzamidine were purchased from Sigma Chem. Co. (St. Louis, MO). Ammonium chloride was from Fisher Scientific Co. (Fairlawn, NJ). PMSF was from Boehringer Mannheim GmbH (Germany). DTT and paraformaldehyde were from Fluka Chemical Corp. (Ronkonkoma, NY). SDS was from Pierce (Rockford, IL). n-Octyl-β-D-glucopyranoside (octyl-glucoside) was from Calbiochem Co. (La Jolla, CA). Monoclonal anti-DNP IgG was from Oxford Biomedical Research (Oxford, MI). Goat anti-rabbit IgG conjugated to gold (10 nm) was from Biocell Research Laboratories (Ted Pella, Redding, CA). ^{125}I-conjugated to goat anti-rabbit IgG and goat anti-mouse IgG and [^{125}I]streptavidin were from Amersham Corp. (Arlington Heights, IL). [α-^{32}P]GTP was from DuPont New England Nuclear Co. (Boston, MA). Biotinylated horse anti-mouse serum and horse serum were from Vector Labs. (Burlingame, CA). Alkaline phosphatase-conjugated goat anti-rabbit or goat anti-mouse IgG and BCIP/NBT alkaline phosphatase substrate system were from Bio-Rad Labs. (Hercules, CA). Phosphatidylinositol specific phospholipase C (PI-PLC) was from ICN Biochemicals Co. (Cleveland, OH). Monoclonal anti-caveolin IgG (20B) was kindly provided by Dr. J. Glenney (University of Kentucky, Lexington). The following antisera against heterotrimeric G proteins were prepared as previously described (29): anti-$G_{\alpha s}$ (584), anti-$G_{\alpha i1/\alpha i2}$ (BO87), anti-$G_{\alpha i3}$ (C-260), and anti-Gβ (B-600). An affinity purified anti-peptide antibody against RaplA/B was prepared as previously described (4, 25). An antibody that recognizes a common epitope [Cross Reacting Determinant (CRD)] exposed on all GPI-anchored membrane proteins after release from the membrane by PI-PLC was prepared as previously described (15).

Buffers used were prepared according to the following formulas: (buffer A) 50 mM MOPS, 150 mM NaCl, 5 mM EDTA, 5 mM EGTA, 0.05% sodium azide, pH 7.1, 1 mM DTT, 10 μM leupeptin, 0.5 mM benzamidine, 10 μg/ml soybean trypsin inhibitor, 1 μg/ml pepstatin A, 1 mM PMSF. (buffer B) 0.25 M sucrose, 10 mM Tris, 5 mM EDTA, 5 mM EGTA, 0.05% sodium azide, pH 7.1, 1 mM DTT, 10 μM leupeptin, 0.5 mM benzamidine, 10 μg/ml soybean trypsin inhibitor, 1 μg/ml pepstatin A, 1 mM PMSF. (buffer C) 2 M sucrose, 10 mM Tris, 5 mM EDTA, 5 mM EGTA, 0.05% sodium azide, pH 7.1, 1 mM DTT, 10 μM leupeptin, 0.5 mM benzamidine, 10 μg/ml soybean trypsin inhibitor, 1 μg/ml pepstatin A, 1 mM PMSF. (buffer D) 50 mM MOPS, 300 mM NaCl, 5 mM EDTA, 5 mM EGTA, 0.05% sodium azide, pH 7.1, 1 mM DTT, 10 μM leupeptin, 0.5 mM benzamidine, 10 μg/ml soybean trypsin inhibitor, 1 μg/ml pepstatin A, 1 mM PMSF. (buffer E) 2.3 mM NaH_2PO_4-H_2O, 7.7 mM Na_2HPO_4-$7H_2O$, 150 mM NaCl, 2 mM $MgCl_2$, pH 7.4. (buffer F) buffer E plus 2 mg/ml heat-denatured BSA (80°C, 3 min). (buffer G) buffer E plus 0.2 mg/ml heat-denatured BSA. (buffer H) buffer E plus 2 mg/ml heat-denatured BSA and 2% horse serum. (buffer I) 50 mM Tris, pH 8.0, 2 mM $CaCl_2$, 80 mM NaCl. (buffer J) buffer I plus 5% nonfat dry milk, 0.2% (vol/vol) NP-40, 0.02% sodium azide. (buffer K) 50 mM Tris, pH 7.5, 300 mM NaCl. (buffer L) buffer K plus 3% fish gelatin. (buffer M) buffer K plus 1% fish gelatin. (buffer N) 50 mM Tris-HCl, 0.3% Tween 20, 5 mM $MgCl_2$, 1 mM EGTA, pH 7.5. (buffer O) 100 mM phosphate buffer, pH 7.4. (buffer P) buffer O containing 0.1% BSA, 0.02% sodium azide, and 0.05% saponin. (buffer Q) buffer O containing 0.1% BSA.

Methods

Purification of Caveolae. The purification scheme is shown in Fig. 1. All steps were carried out at 4°C. A plasma membrane fraction from chicken gizzard was prepared by a modification of the methods reported by Lucchesi et al. (28) and Hubbard et al. (16). One hundred grams of gizzard was excised, trimmed of connective tissue, and minced in 0.25 L of buffer A in a Waring blender for 30 s. The minced tissue was further homogenized with 2 × 30 s in a Waring blender in a total of 1 L of buffer A. Finally the sample was homogenized in a polytron homogenizer (Brinkman Instruments Inc., Westbury, NY) for 2 × 30 s at 27,000 rpm. The crude homogenate was centrifuged for 20 min at 5,000 *g* to obtain the *Starting Material*. This was filtered through four layers of gauze before being used to prepare caveolae.

A small portion of the *starting material* was centrifuged at 100,000 *g* for 1 h and designated as the *total membrane* fraction (see Fig. 5). The remaining *starting material* was centrifuged for 10 min at 10,000 *g* to remove any aggregated material (Pellet A). *Supernatant A* was filtered through 12 layers of gauze, adjusted to 1 M KCl and stirred for 30 min. The mixture was centrifuged for 90 min at 30,000 *g*. *Pellet B* was resuspended in buffer B by 10 up-and-down strokes of a tight-fitting dounce homogenizer. Two volumes of buffer C were added to the homogenate (final concentration of sucrose 1.42 M) and 35-ml aliquots were added to each centrifuge tube. Each sample was overlaid with 2 ml buffer B (sucrose concentration, 0.25 M) and centrifuged for 60 min at 82,000 *g* in a Beckman SW 28 rotor at 4°C. The .25/1.4 M interface (*Membrane I*) was collected with a blunt-tipped Pasteur pipette and resuspended in buffer A by 10 strokes of a tight-fitting dounce homogenizer. This suspension was mixed with an equal volume of 4 M KI (freshly prepared in buffer A) and stirred for 30 min. 36-ml aliquots of the sample were added to centrifuge tubes and centrifuged for 60 min at 100,000 *g* in a Beckman SW 28 rotor. A brownish, membrane pellicle formed at the top of 2 M Kl (*Membrane II*), which was collected with a blunt-tipped Pasteur pipette and resuspended by 10 strokes of the tight dounce homogenizer in buffer D and stored at 4°C.

Membrane II, which corresponded to the plasma membrane fraction, was mixed with an equal volume of 2.5 M sucrose to a final concentration of 42%. 4-ml aliquots of the sample (7-10 mg proteins) were added to centrifuge tubes, and then overlaid with 8 ml of 25% sucrose followed by 5 ml of 15% sucrose. The samples were then centrifuged for 2 h at 100,000 *g*. A cloudy material accumulated at the interface between both the 15–25% and the 25–42% sucrose layers. The 15–25% sucrose interface plus the 25% sucrose fraction were pooled, diluted in two times volume of buffer D and concentrated by centrifuging onto 42% sucrose cushion for 1 h at 100,000 *g*. The pellicle on the cushion (*Membrane III*) was resuspended by 10 strokes of a tight-fitting dounce homogenizer in buffer D.

Membrane III was adjusted to a protein concentration of 4–5 mg/ml with buffer D, with equal volume of 1% Triton X-100 (final Triton concentration 0.5% in buffer D) and incubated for 30 min with constant rocking. A sucrose step gradient was prepared using 0.5% Triton X-100 in buffer D that consisted of 1.5 ml of 42% sucrose, 3 ml 25% sucrose, and 3.5 ml 15% sucrose. Two ml of Triton X-100 treated Membrane III was layered on the top of the sucrose gradient and centrifuged for 2 h at 100,000 *g*. The 15–25% sucrose interface (*Membrane IV*) was collected and washed with 0.1 M sodium carbonate before centrifuging for 1 h at 100,000 *g* onto a 42% sucrose cushion. The pellicle on the cushion was collected, resuspended in buffer A, and stored at −80°C. This fraction was designated *caveolae*.

Radioimmunoassay. After protein measurement, samples were first dissolved in 60 mM octyl-glucoside in water, and then diluted to desired concentration in water. Aliquots of the sample (10 ng) were placed in individual wells of an Immuno 2, 96-well plate (Dynatech Lab, Inc., Chantilly, VA) and air-dried overnight. The wells were washed three times with buffer E, and then incubated in the presence of buffer F for 1 h at 37°C. The wells were washed an additional three times with buffer G before adding 50 μl of the anti-caveolin IgG (2 μg/ml in buffer H) to the wells and incubating for 1 h at 37°C. Each well was washed seven times with buffer G before adding 50 μl of biotinylated, horse anti-mouse IgG (2 μg/ml in buffer H) and incubating for 1 h at 37°C. The wells were washed seven times with buffer G before 50 μl of [^{125}I]streptavidin (2 μCi/ml in buffer F, preadsorbed with Dowex resin to remove free ^{125}I; Sp. Act. = 20–40 μCi/μg) was added to

wells and incubated for 15 min at room temperature with constant rocking. The wells were washed a final seven times with buffer G before being placed into a 12 × 75 mm tube and counted in a Packard Cobra II Gamma counter (Packard Ins. Co., Meriden, CT).

Electrophoresis and Immunoblot. Most of the samples were dissolved in sample buffer (23) and heated for 3 min at 100°C before being loaded onto gels. Samples for heterotrimeric G protein analysis were prepared by a modification of the method of Sternweis and Robinshaw (49). Protein samples (20 μl) were mixed with 5 μl of 10% SDS/1 mM DTT, followed by heating for 5 min at 100°C. The samples were then cooled to room temperature. A 5-μl aliquot of 0.3 M NEM (N-ethylmaleimide) was added to each sample and incubated for 10 min at room temperature. A 10-μl aliquot of 4× SDS sample buffer was then added to the samples and heated for 3 min at 100°C before loading on gels.

Proteins were separated by SDS-PAGE using the method of Laemmli (23). Proteins separated on the indicated percent gels were electrophoretically transferred to nitrocellulose membrane (pore size, 0.45 μm) by the method of Towbin (51). Transfer was performed at a 100 V for 60 min at 4°C using a solution containing 20% methanol, 0.025 M Tris, and 0.192 M glycine (pH 8.5) as the electrode buffer.

[^{125}I] IgG Blots. Nitrocellulose membranes were rinsed briefly with buffer I and incubated with buffer J for 1 h at room temperature. They were then incubated with the indicated concentration of primary antibody (diluted in buffer J) for 1 h at room temperature or overnight at 4°C. The blots were washed three times for 15 min in buffer J, and then incubated with either ^{125}I-conjugated goat anti-mouse IgG or goat anti-rabbit IgG at 5×10^5 cpm/ml (sp. act., 20 μCi/μg of protein) in buffer J for 1 h at room temperature. The blots were washed three times for 15 min in buffer J, rinsed two times in buffer I, and then washed two times for 10 min in buffer I. Antibody binding was visualized by autoradiography using Kodak X-OMAT AR film.

Alkaline Phosphatase BCIP/NBT Blots. Nitrocellulose membranes were rinsed briefly with buffer K and incubated with buffer L for 1 h at room temperature. The blots were then incubated with the indicated concentration of primary antibody (diluted in buffer M) for 1 h at room temperature or overnight at 4°C. The blots were washed three times for 5 min in buffer M, and then incubated with alkaline phosphatase-conjugated to either goat anti-mouse IgG (1:2,000 dilution in buffer M) or goat anti-rabbit IgG (1:2,000 dilution in buffer M) for 2 h at room temperature. The blots were washed three times for 5 min in buffer K, and then processed to visualize the bands using the BCIP/NBT alkaline phosphatase substrate system.

[α-^{32}P]GTP Binding. [α-^{32}P]GTP binding was carried out according to the method of Lapetina and Reep (24). The nitrocellulose containing transferred proteins was rinsed briefly in buffer N. The nitrocellulose was then incubated for 90 min at room temperature with [α-^{32}P]GTP in buffer N (1 μCi/ml; specific activity, 3,000 Ci/mmol) in the absence or presence of 1 μM GTP. The blots were rinsed with several changes of buffer N over 1~2 h and air-dried. [α-^{32}P]GTP binding was visualized by autoradiography using Kodak X-OMAT AR film.

PI-PLC Treatment. PI-PLC treatment was carried out using a modification of a method of Lisanti et al. (26). Membrane samples were dissolved in 60 mM octyl-glucoside. The samples were then incubated in the presence or absence of PI-PLC (4 U/ml) for 1 h at 37°C. The reactions were stopped by addition of Laemmli sample buffer and boiled for 3 min. The samples were subjected to SDS-PAGE and transferred to nitrocellulose paper.

Immuno-Gold Labeling of Thin Sections. Fresh chicken gizzard was fixed overnight in 3% (wt/vol) paraformaldehyde in buffer O containing 3 mM trinitrophenol, 4 mM KCl, and 2 mM $MgCl_2$. Vibratome sections (60–80 μm thick) of the fixed chicken gizzard were prepared and washed in buffer O containing 100 mM NH_4Cl for 30 min. The sections were then rinsed twice with buffer O and incubated in buffer P for 1–3 h at room temperature. Primary antibodies, mouse monoclonal anti-caveolin IgG (designated 20B), and irrelevant mouse monoclonal IgG (designated 2001) were diluted in buffer P to a final concentration of 30 μg/ml. Groups of 6–8 sections were incubated overnight with each of the primary antibodies. This was followed by an 8-h incubation in the presence of 25 μg/ml of goat anti-mouse IgG conjugated to DNP in buffer P. Sections were washed after each incubation three times for 10 min each in buffer P. After a final wash, sections were rinsed twice in buffer O, fixed with 1% glutaraldehyde for 2 h in buffer O, washed with buffer O containing 100 mM NH_4Cl for 30 min, and rinsed twice in buffer O. Tissue sections were post fixed with 1% osmium tetroxide in buffer O for 2 h, dehydrated, embedded in Epon, sectioned, and processed to localize DNP groups by immunogold labeling as previously described (34).

Immuno-Gold Labeling of Fractions. Samples from purified fractions were mixed with an equal volume of 120 mM octyl-glucoside for 10 min on ice without vortexing to dissociate aggregates. This was followed by fixation with 3% paraformaldehyde in buffer O for 10 min. The fixed samples (2–3 μl) were air-dried onto carbon-coated grids. The grids were washed in buffer O followed by incubation with 100 mM NH_4Cl (in buffer O) for 30 min and buffer Q for 30 min. All the antibodies were diluted in buffer Q. The grids were incubated 30 min each with primary antibodies (20 μg/ml) followed by 50 μg/ml of either goat anti-mouse IgG or goat anti-rabbit IgG and finally a 1:30 dilution of gold-conjugated rabbit anti-goat IgG. The grids were washed after each incubation three times for 30 min in buffer Q. After a final wash, grids were rinsed twice in buffer O, post fixed with 1% osmium tetroxide in buffer O for 10 min and finally stained sequentially for 10 min each with 1% tannic acid, 4% uranyl acetate, and 2% lead citrate.

Other Methods. SDS-PAGE was carried out according to the method of Laemmli (23).

Protein was determined according to Lowry et al. (27) using BSA as a standard.

To measure galactosyltransferase, 10 μg of the indicated membrane fraction was incubated in the presence of 25 mM $MnCl_2$, 2.5 mM mercaptoethanol, 0.08 mg/ml [^{3}H]UDP galactose (sp. act. = 17.2 Ci/mM), 10 mM Hepes-NaOH, pH 7.0 in the absence or presence of 66 mM N-acetylglucosamine at 37°C for 1 h. The reaction was terminated with the addition of 0.3 M EDTA. The product (N-acetyl-lactosamine) was separated on a 1-cm column of Dowex-2-Cl.

The percent of the cell surface occupied by caveolae was determined by: measuring the average diameter of a caveola (75 nm) and using this value to calculate the membrane circumference of a caveola; counting the number of caveolae per linear length of membrane and multiplying this by the caveolar membrane circumference; and dividing total caveolar membrane circumference by the total linear surface counted plus the total caveolar membrane circumference.

Results

Characterization of Purified Caveolae

Caveolin is the only known protein marker for caveolae (39). Immunogold labeling has shown that at the cell surface this protein is found exclusively in caveolae (39). Since caveolin is also found randomly distributed in Golgi membranes (10, 21, 39), our strategy was to prepare plasma membranes from a tissue source that was rich in caveolae and track the purification of the organelle with anti-caveolin IgG. We chose chicken gizzard smooth muscle cells because they have abundant caveolae (Fig. 2 *A*). Immunogold labeling of these cells with the same anti-caveolin IgG that was subsequently used to monitor purification showed that most of the gold labeling was confined to caveolae (Fig. 2, *B* and *C*). We used the typical flask shaped morphology of the caveolar membrane to determine that caveolae represent ~18% of the total surface membrane in these cells. Most likely this is an underestimate because cells contain many uninvaginated caveolae that cannot be detected by thin section electron microscopy (39).

We developed a purification protocol that requires three steps (Fig. 1): preparation of plasma membranes stripped of peripheral membrane proteins (Membrane II); enrichment for light plasma membranes on a sucrose step gradient (Membrane III); and treatment of light plasma membranes with Triton X-100 followed by separation of soluble from insoluble material on a sucrose gradient (Membrane IV). We measured the specific activity of caveolin in each fraction using a radioimmune assay for bound anti-caveolin IgG. The specific activity (*A*) and the protein profile (*B*) of the various fractions obtained in a typical purification run is shown in Figs. 3 and 4. The starting material had significant activity, but when we separated the plasma membrane from the cytosol, most of this activity fractionated with the membrane

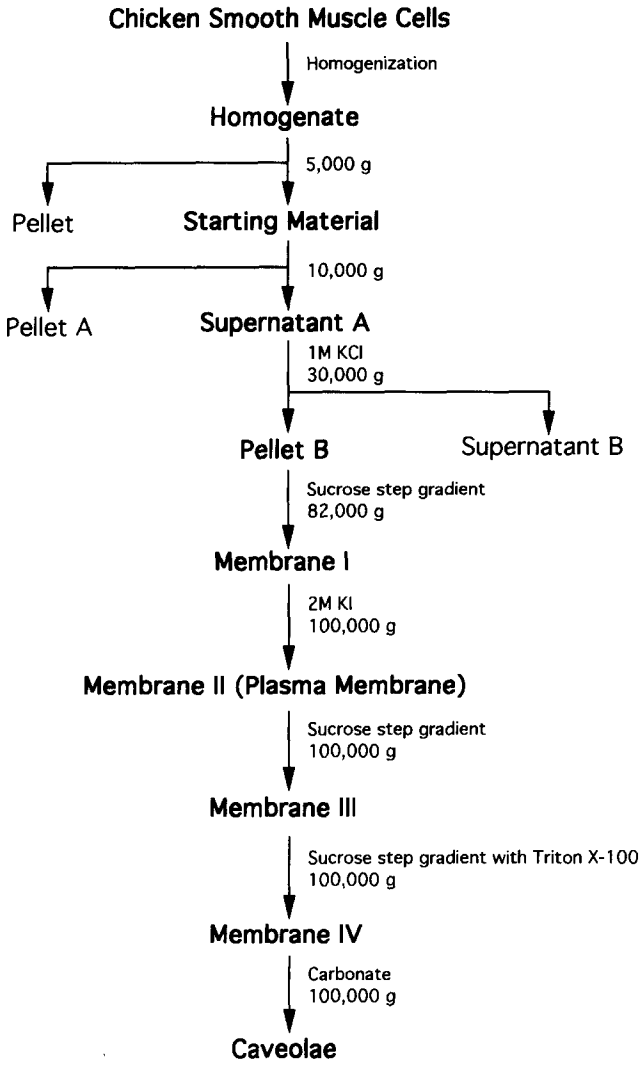

Figure 1. Diagrammatic representation of the protocol used to purify caveolae from chicken gizzard smooth muscle.

(data not shown). Fig. 3 shows that when Membrane II was loaded onto a sucrose step gradient and centrifuged at 100,000 *g* for 2 h, the membranes at the 15%/25% interface had the highest caveolin specific activity. The 25% fraction had nearly the same activity, but the other fractions were quite low. We pooled the two fractions with the highest activity, treated them with 0.5% Triton X-100 (2–3 mg of protein in each treatment) and loaded the material onto a second sucrose step gradient (Fig. 4). The 15%/25% interface in this gradient had the highest activity, with a 1.8-fold increase over the Membrane III. Very little material was recovered in the denser fractions (data not shown). We washed the 15%/25% interface with carbonate and designated it the caveolae fraction. From 100 g wet weight of tissue, we obtained 1.5 mg of protein in the caveolae fraction. This fraction contained 1–5% of the caveolin present in the starting material.

The above assay indicated that, compared to the plasma membrane fraction, there was ~5-fold enrichment in caveolin in the caveolae fraction. To further assess the purity of the caveolae preparation, we analyzed four different fractions by both polyacrylamide gel electrophoresis (Fig. 5 *A*) and immunoblotting using anti-caveolin IgG (Fig. 5 *B*). We could identify at least 30 different bands that copurified with caveolae. The most prominent proteins are indicated by the arrowheads and caveolin by the arrow (Fig. 5 *A*). By immunoblotting (Fig. 5 *B*), three caveolin-specific bands (apparent *MW*; 22,000, 24,000, and ~300,000) were most intense in the caveolae fraction. The high molecular weight band corresponds to a polymer of caveolin (14) while the two low molecular weight bands are isoforms of monomeric caveolin. Scanning densitometry of the caveolin-specific bands in the immunoblots indicated that caveolin was enriched ~5-fold in the caveolae fraction relative to the plasma membrane and ~200-fold relative to the whole tissue starting material (Fig. 1).

Another test of the purification scheme is to show that marker proteins for other compartments are excluded from the caveolae fraction. Fig. 5 *A* documents that multiple, Coomassie blue positive bands were excluded as caveolae were purified. The pattern also indicates that many of the proteins in the plasma membrane were not present in the caveolae fraction (compare plasma membrane lane with caveolae lane). We also measured the activity of galactosyltransferase, a marker for Golgi membranes. The activity in pellet B was 22,747 cpm/min/mg of protein, which was comparable to the activity of a control Golgi fraction isolated from rat liver (17,993 cpm/min/mg). By contrast, the activity in the caveolae fraction was not above background (1,609 cpm/min/mg of protein). Therefore, Golgi membranes did not contaminate the caveolae fraction. Finally, we used immunoblotting to measure the concentration of the cytoplasmic protein, annexin VI. This protein was excluded from caveolae (data not shown).

GPI-anchored membrane proteins are another marker for caveolae. Immunogold electron microscopy has shown that nearly every caveola is associated with a cluster of GPI-anchored proteins. On the other hand, the caveolae-associated clusters only represent ~18% of the total number of GPI clusters on the cell surface (54). We used a polyclonal antibody that recognizes the cross-reacting determinant (CRD) epitope exposed when GPI-anchored proteins are released from membranes by PI-PLC (15) to determine if GPI-anchored proteins were enriched in the caveolae fraction (Fig. 6, *A* and *B*). Immunoblots with this antibody detected at least nine different GPI-anchored membrane proteins that were highly enriched (Fig. 6, *A* and *B*). When we quantified the more intense bands by scanning densitometry we found that these GPI proteins were enriched 13–18-fold in the caveolae fraction relative to the plasma membrane.

We next used whole mount electron microscopy and immunogold cytochemistry to characterize the morphology of the membranes in the caveolae fraction (Fig. 7). Samples of the fraction were fixed, dried down onto the surface of a formvar-coated grid, and positively stained with heavy metals (Fig. 7 *A*). These fractions typically contained numerous, cup-shaped pieces of membrane. At higher magnification (Fig. 7 *A*, *inset*), these cups appeared to be partially decorated by a striated coat. We also saw smaller pieces of membrane interspersed between the cup profiles. These appeared to be fragments of caveolae because they contained remnants of the coat material and were positive for anti-caveolin IgG binding by immunogold cytochemistry (Fig. 7 *B*). Nearly all of the membrane fragments, plus the cup-shaped segments,

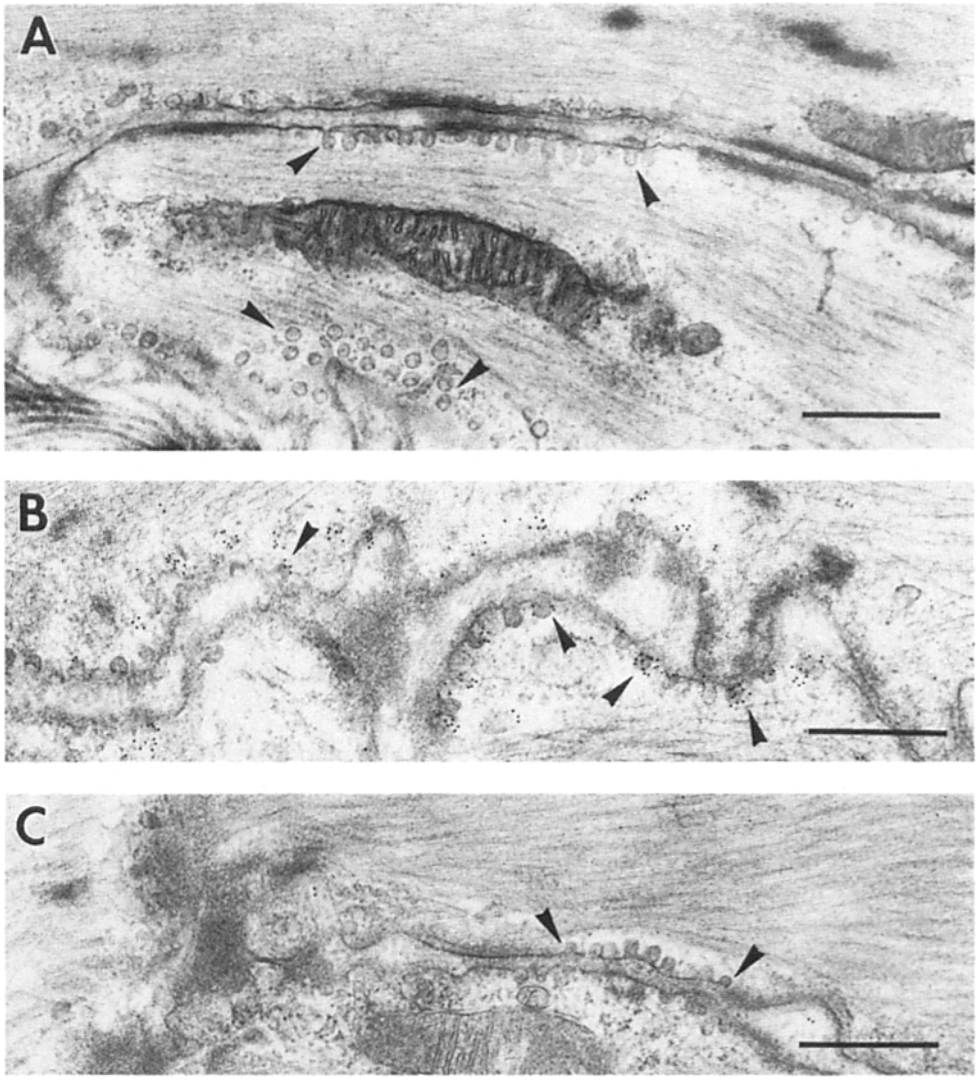

Figure 2. Electron microscopic visualization of chicken smooth muscle cells that were either unprocessed (*A*) or processed (*B* and *C*) to localize caveolin by immunogold cytochemistry. Fresh chicken gizzard was either fixed directly and embedded for electron microscopy (*A*) or fixed and processed to localize caveolin using either a monoclonal anti-caveolin IgG (*B*) or an irrelevant monoclonal IgG (*C*) as described. Arrowheads indicate caveolae. Bar, 0.5 μm.

decorated with anti-caveolin IgG. A high magnification view shows how the gold was often associated with the striated coat (Fig. 7 *B, inset*). We did not see any gold labeling when an irrelevant monoclonal IgG was substituted for monoclonal anti-caveolin IgG (Fig. 7 *C*).

GTP-binding Proteins Are Enriched in Caveolae

Sargiacomo et al. (43) recently reported that both small and heterotrimeric GTP-binding proteins coenrich with caveolin in Triton X-100 insoluble, membrane fractions prepared from tissue culture cells. We used specific antibodies to see if any of these regulatory proteins were also associated with smooth muscle caveolae. We used mono-specific peptide antibodies against various GTP-binding proteins to immunoblot the indicated fractions. Fig. 8 shows that both $G_{\alpha s}$ (Fig. 8 *A*) and $G_{\alpha i3}$ (Fig. 8 *B*) are enriched in caveolae. Scanning densitometer reading of the blots indicated that the specific blotting activity of $G_{\alpha s}$ was increased eightfold compared to plasma membranes while $G_{\alpha i3}$ was increased sixfold. An antibody that recognizes both $G_{\alpha i1}$ and $G_{\alpha i2}$ showed that these subunits were also enriched (~3-fold) in the caveolae fraction (Fig. 9 *A*). When we used this antibody to immunogold label the caveolae fraction (Fig. 9 *B*), many of the caveolae profiles were heavily decorated with gold. Immunogold labeling was not seen when a preimmune IgG was substituted for the anti-$G_{\alpha i1}/G_{\alpha i2}$ IgG (data not shown).

In contrast to the G_α subunits, the specific blotting activity of the G_β subunit indicated that this subunit was no more concentrated in caveolae than in the starting material (compare *starting material* with *caveolae*, Fig. 10 *A*) even though there was some enrichment in the plasma membrane fraction. Immunoblot analysis of each fraction obtained during the purification showed that Triton X-100 removed G_β from the Membrane III fraction (data not shown). Therefore, we used immunogold electron microscopy to determine if G_β was present in caveolae before detergent treatment (Fig. 10, *B*, *C*, and *D*). The light membrane fraction obtained before detergent treatment (Membrane III, Fig. 10 *C*) had many cup-shaped membrane profiles that decorated with the anti-G_β IgG gold probe (*arrows*, Fig. 10 *C*). By contrast, we found substantially less gold associated with similar appearing pieces of membrane in the detergent-treated fraction (Membrane IV, Fig. 10 *D*). We verified that the labeled segments of membrane in Membrane III were caveolae by colocalizing both caveolin (large gold, Fig. 10 *B*) and G_β

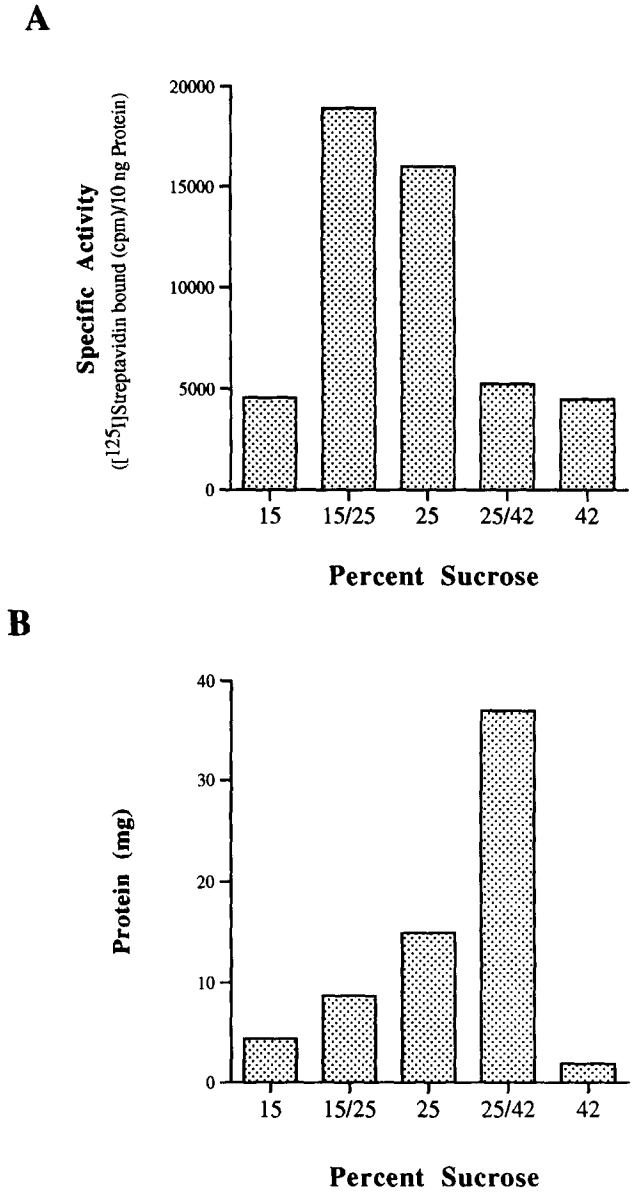

Figure 3. The specific activity of caveolin (*A*) and the protein distribution (*B*) in fractions obtained from the first sucrose step gradient. Membrane II was mixed with 2.5 M sucrose to a final concentration of 42%, overlaid with a 15%–25% sucrose step gradient, and centrifuged at 100,000 *g* for 2 h at 4°C. The gradient was divided into five fractions: 15%; the 15/25% interface; 25%; the 25/42% interface; and 42% sucrose. Each fraction was assayed for the presence of caveolin using a radioimmune assay as described. The 15/25% interface and the 25% fraction were pooled and designated Membrane III.

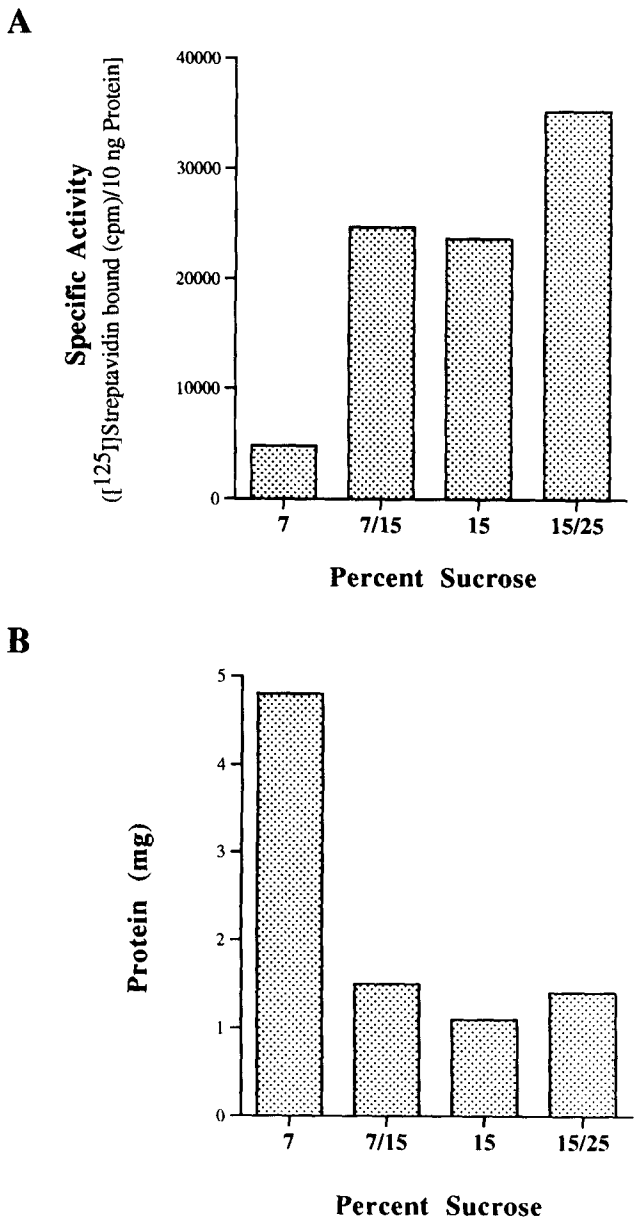

Figure 4. The specific activity of caveolin (*A*) and the protein distribution (*B*) in fractions obtained from the second sucrose gradient. Membrane III was adjusted to a protein concentration of 4–5 mg/ml with buffer F, adjusted to 0.5% Triton X-100, and incubated for 30 min, all at 4°C. The sample was then loaded on the top of a sucrose step gradient and centrifuged at 100,000 *g* for 2 h at 4°C. The gradient was divided into four fractions: 7%; the 7/15% interface; 15%; and the 15/25% interface. Each fraction was assayed for the presence of caveolin using a radioimmune assay as described. The 15/25% interface was designated Membrane IV.

(small gold, Fig. 10 *B*) to the same pieces of membrane. Therefore, caveolae appear to contain both G_α and G_β subunits of the heterotrimeric GTP-binding proteins but that only G_α is detergent resistant.

We also found that several small GTP-binding proteins were enriched in the caveolae fraction (Fig. 11, *A* and *B*). [α-^{32}P]GTP binding to proteins transferred to nitrocellulose revealed two prominent bands that were increased ~2-fold in density compared to plasma membranes. In an effort to identify other GTP-binding proteins, we used a peptide antibody that recognizes RaplA/B to label the caveolae fraction by both immunoblot (Fig. 11 *B*) and immunogold (Fig. 11 *C*). This small GTP-binding protein was enriched ~2-fold in caveolae. Moreover, antibody-specific gold particles sparsely labeled caveolae (Fig. 11 *C*).

Discussion

Caveolae have remained a relatively obscure membrane spe-

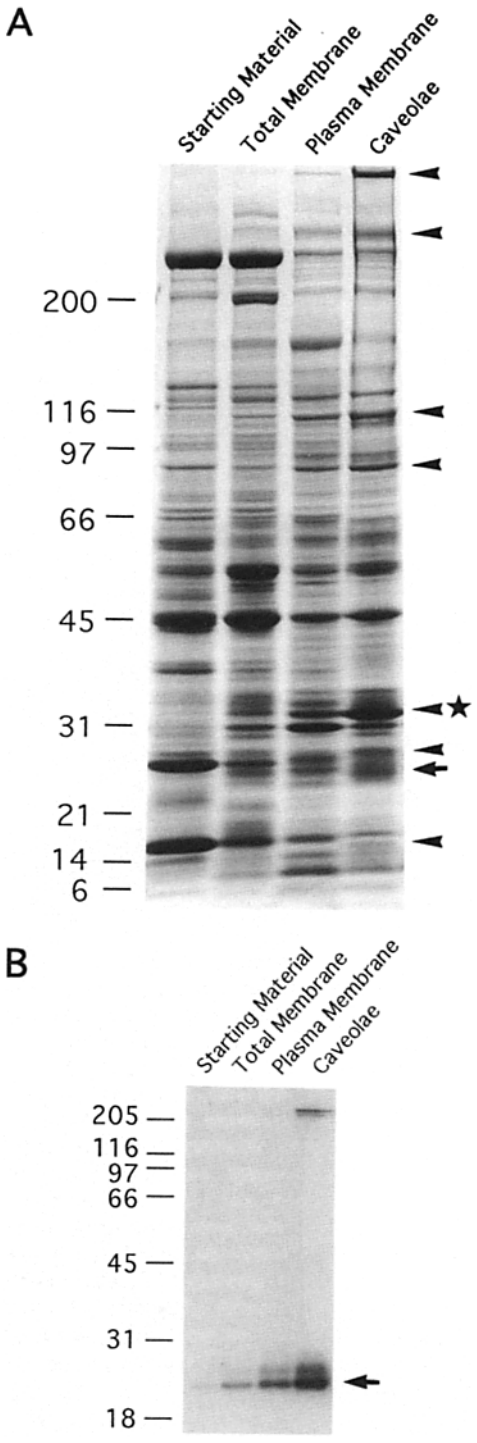

Figure 5. Polyacrylamide gel electrophoresis (*A*) and anti-caveolin IgG immunoblotting (*B*) of different fractions obtained during the purification of caveolae. (*A*) Samples of the indicated fractions (75 μg per lane) were loaded on 6–15% gradient gels, separated by electrophoresis and stained with Coomassie blue as described. The arrow heads indicate proteins that are enriched relative to the plasma membrane. The arrow marks the position of caveolin. The * marks a protein band that appears to be more abundant in caveolae than caveolin. (*B*) Samples of the indicated fractions (5 μg per lane) were loaded on gels, separated by electrophoresis (11% gel) and transferred to nitrocellulose for blotting with anti-caveolin IgG (15 μg/ml). Anti-caveolin was detected using an ^{125}I-labeled goat anti-mouse IgG. The arrow indicates the caveolin band.

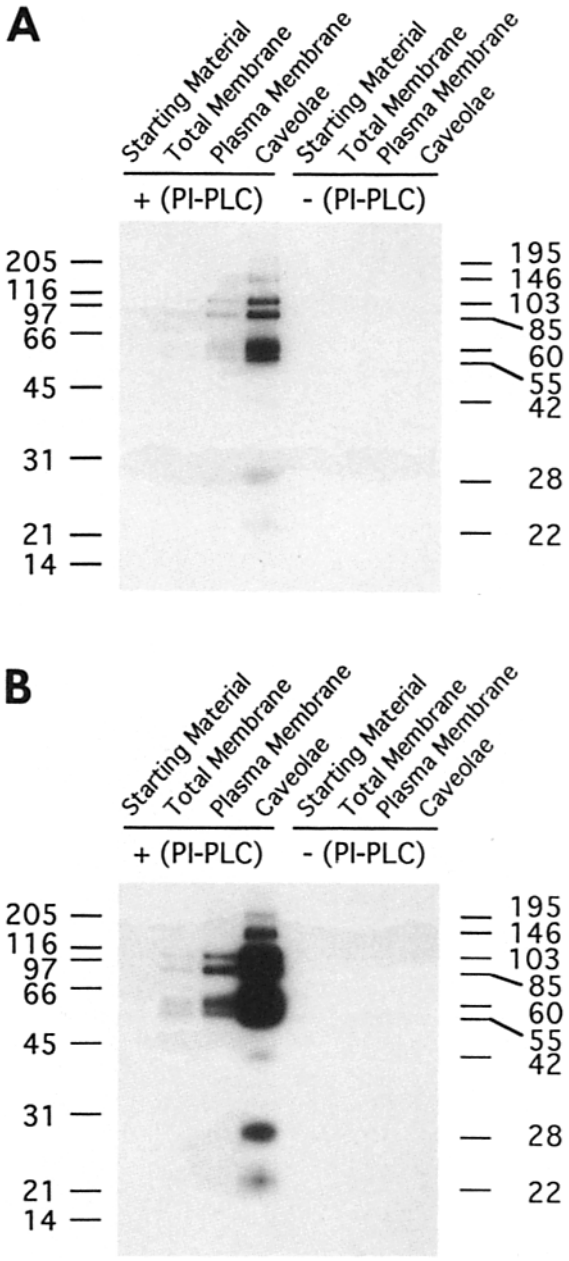

Figure 6. Purified caveolae are enriched in multiple GPI anchored membrane proteins. Samples (10 μg) of the indicated fractions were solubilized in 60 mM octyl-glucoside and incubated in the presence (+) or absence (−) of PI-PLC for 1 h at 37°C. Each sample was then separated on an 11% gel by electrophoresis and immunoblotted with rabbit anti-CRD IgG (serum) using ^{125}I-goat anti-rabbit IgG as described. An overnite (*A*) and a 3-d (*B*) exposure are shown.

cialization since their identification as a flask-shaped invagination on the surface of epithelial (53) and endothelial cells (32) nearly 40 years ago. A full scale investigation into the structure and function of caveolae could not proceed until there was a method available for obtaining large quantities of the organelle. Two advances have now made this possible: the identification of a resident, integral membrane protein of caveolae called caveolin (39), and the discovery that each caveola contains a cluster of GPI-anchored membrane pro-

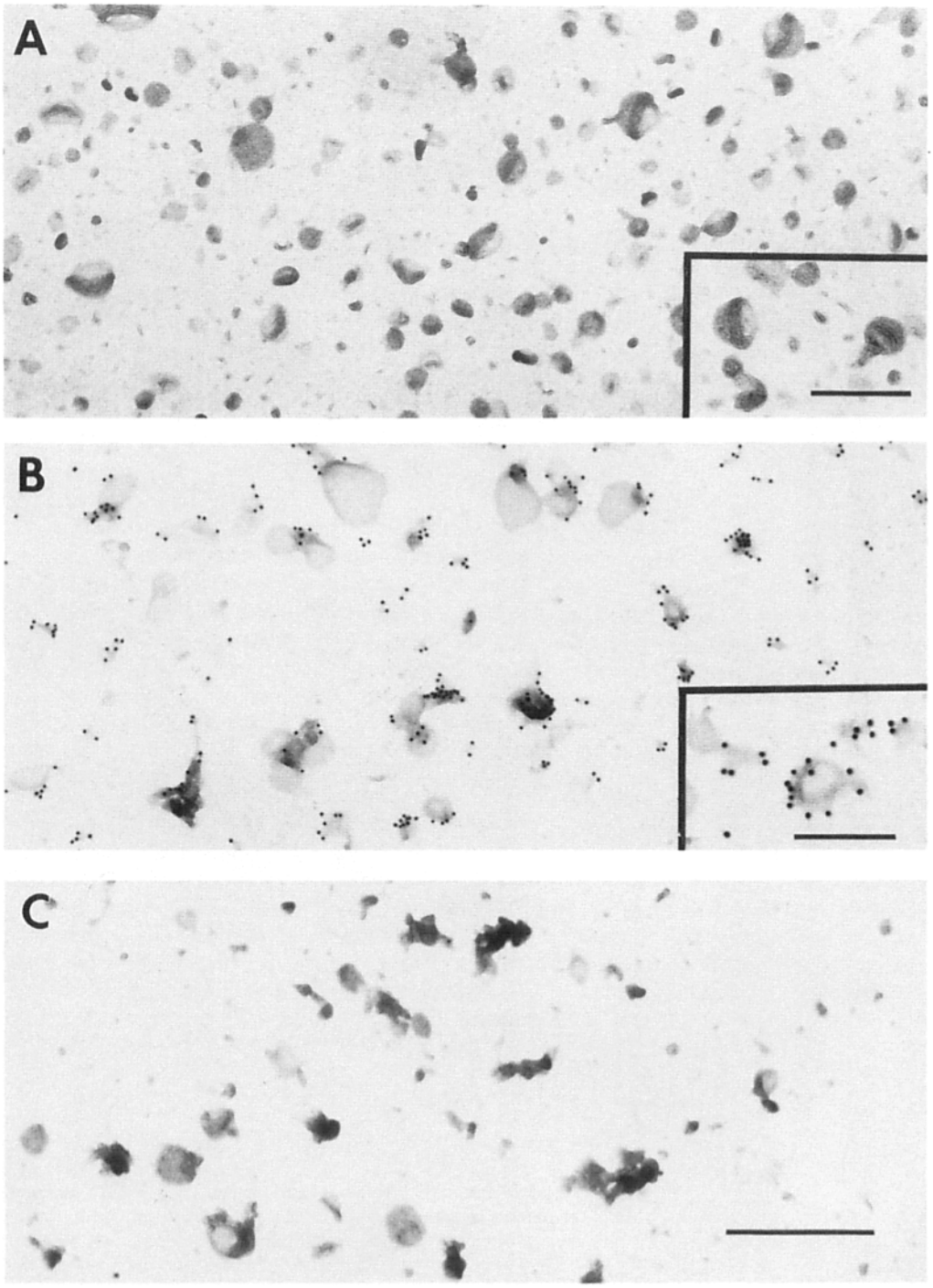

Figure 7. Whole mount electron microscopic visualization of untreated, purified caveolae (*A*) or purified caveolae labeled by immunogold with either anti-caveolin IgG (*B*) or irrelevant IgG (*C*). Samples of Membrane IV were briefly treated with octyl-glucoside on ice, fixed, and air-dried onto grids. The grids were then either viewed directly (*A*) or processed to localize anti-caveolin IgG binding sites (*B*) or non-immune IgG binding sites (*C*). Bar, 0.3 μm (*inset*, 0.2 μm).

teins (41). We have used the relative enrichment of these markers as a guide for purification.

In any purification scheme a question always arises about the purity of the final preparation. A linear measure of the plasma membrane indicates that caveolae make up ~18% of the surface of chicken gizzard smooth muscle cells. If all of the non-caveolar membrane was removed from the plasma membrane, then a 5.5-fold enrichment for the caveolae segment is all that is needed for a complete purification. We used both a radioimmune assay for caveolin and whole mount electron microscopy to monitor purification. Anti-caveolin IgG was useful for monitoring caveolae behavior during the fractionation, but we could not use this marker to determine purity because we do not know the specific concentration of caveolin in each caveolae or whether all caveolae have caveolin. Therefore, we used electron microscopy to examine the fractions with the highest caveolin specific activity and found that the principal membrane component had the morphological characteristics of caveolae. Moreover, nearly all of the membrane profiles in these preparations decorated with anti-caveolin IgG gold particles (Fig. 7). Therefore, these fractions contain relatively pure caveolae

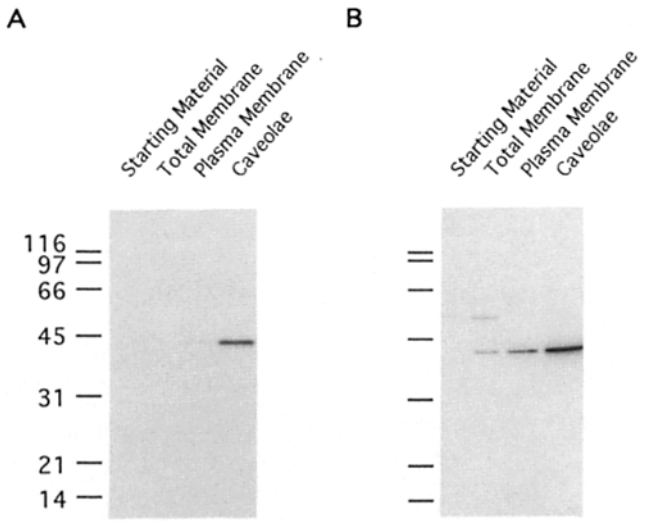

Figure 8. Immunoblot detection of either $G_{\alpha s}$ (*A*) or $G_{\alpha i3}$ (*B*) in different fractions obtained during the purification of caveolae. Samples (5 μg) of the indicated fraction were separated by electrophoresis on 11% polyacrylamide gels and immunoblotted with polyclonal peptide antisera against either $G_{\alpha s}$ (*A*) or $G_{\alpha i3}$ (*B*) using ^{125}I-goat anti-rabbit IgG to detect the rabbit IgG.

even though caveolin is enriched only ~5-fold relative to the plasma membrane.

In contrast to caveolin, GPI-anchored membrane proteins were enriched ~15-fold in the caveolae fraction. The anti-CRD IgG detected at least nine bands on immunoblots. Scanning densitometry of the four most prominent bands showed that they were enriched from 13–18-fold. The relative enrichment was independent of the band intensity. This suggests that the GPI-anchored proteins are purifying as a unit but that there are variable amounts of the individual proteins within the unit. These findings are consistent with electron microscopic studies showing that caveolae contain clusters of GPI-anchored proteins composed of multiple protein species (54).

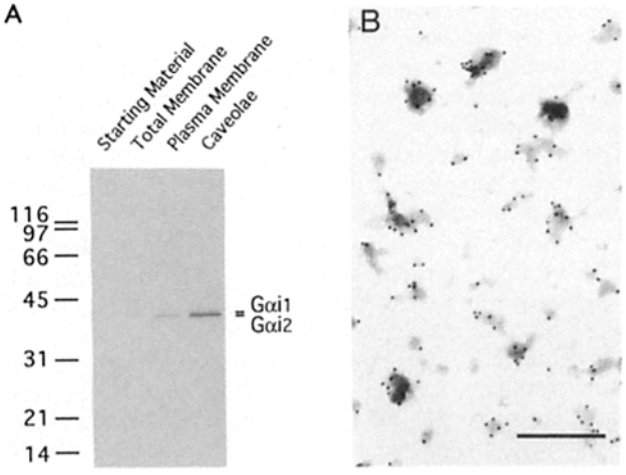

Figure 9. Immunoblot (*A*) and immunogold (*B*) localization of $G_{\alpha i1}/G_{\alpha i2}$ in fractions obtained during the purification of caveolae. (*A*) Samples (5 μg) of the indicated fraction were separated by electrophoresis on 11% polyacrylamide gels and immunoblotted with polyclonal peptide antisera (1:2,000 dilution) against $G_{\alpha i1}/G_{\alpha i2}$ using ^{125}I-goat anti-rabbit IgG to detect the rabbit IgG. (*B*) The caveolae fraction was processed for whole mount immunogold labeling with anti-$G_{\alpha i1}/G_{\alpha i2}$ antisera (*B*) using an antibody sandwich that consisted of, goat anti-rabbit IgG followed by gold-conjugated rabbit anti-goat IgG. Bar, 0.3 μm.

An analysis of the polyacrylamide gel staining pattern for purified caveolae shows that they contain a complex mixture of proteins. Relative to the plasma membrane, many proteins are enriched, some are excluded, and still others are present at the same concentration (compare bands present in plasma membrane lane with those in the caveolae lane, Fig. 5). We determined by immunoblot and immunogold labeling (data not shown) that one of the proteins in the last category is actin (at the 45-kD marker, Fig. 5 *A*). Despite the harsh salt and detergent treatments, actin remained bound to caveolae throughout the purification. This association may be due to the presence of a high affinity, actin-binding protein in caveolae or simply be the consequence of a non-specific interaction. Nevertheless, these results point out that many of the proteins that are not enriched may still be legitimate components of the organelle. By contrast, the enriched bands probably correspond to proteins that carry out a specific cellular function in caveolae. At least one of these proteins (★, Fig. 5 *A*) appeared to be more abundant than caveolin. This raises the possibility that caveolae contain other structural proteins besides caveolin. Future sequence analysis may help to determine a function for these proteins.

Sargiacomo et al. (43) recently reported that heterotrimeric GTP-binding proteins are associated with caveolin-rich domains isolated from tissue culture cells. Furthermore, immunocytochemical studies have found that G_{α} colocalizes with caveolin in MA 104 cells (Mumby, S. M., Q. Yang, H. K. Hagler, A. G. Gilman, and K. H. Muntz, unpublished observations). We found that smooth muscle cell caveolae are also enriched in these proteins. Peptide antibodies that recognize different G_{α} subunits were used to monitor the specific blotting activity of each subunit during caveolae purification. Depending on the subunit, activity was found to increase from 3 to 8-fold relative to the plasma membrane. Immunogold cytochemistry confirmed that both $G_{\alpha i1}$ and $G_{\alpha i2}$ are associated with isolated caveolae. We also successfully used immunogold cytochemistry to localize the other two G_{α} subunits to caveolae (data not shown).

The caveolae-associated G_{α} most likely corresponds to a subset of all the G_{α} that is associated with the plasma membrane. This subgroup may participate in one or more signaling activities that originate in caveolae. Interestingly, $G_{\alpha s}$ was the least enriched G_{α} found in caveolin-rich domains from MDCK cells (43) but the most enriched subunit in smooth muscle cell caveolae fractions. This suggests that the caveolae found in each type of cell have a unique constellation of G_{α} subtypes that are there to carry out cell-specific signaling functions.

G proteins are largely solubilized from membranes by mild detergents such as Triton X-100. Therefore, the caveolae-associated G_{α} must remain in caveolar membranes during the purification because of a tight interaction with a structural component of the caveolae. $G_{\beta\gamma}$ appears not to hold the G_{α} in place because much of this complex was extracted from partially purified caveolae by Triton X-100. We favor the idea that amino-terminal acylation of G_{α} (25) may control the association with caveolae.

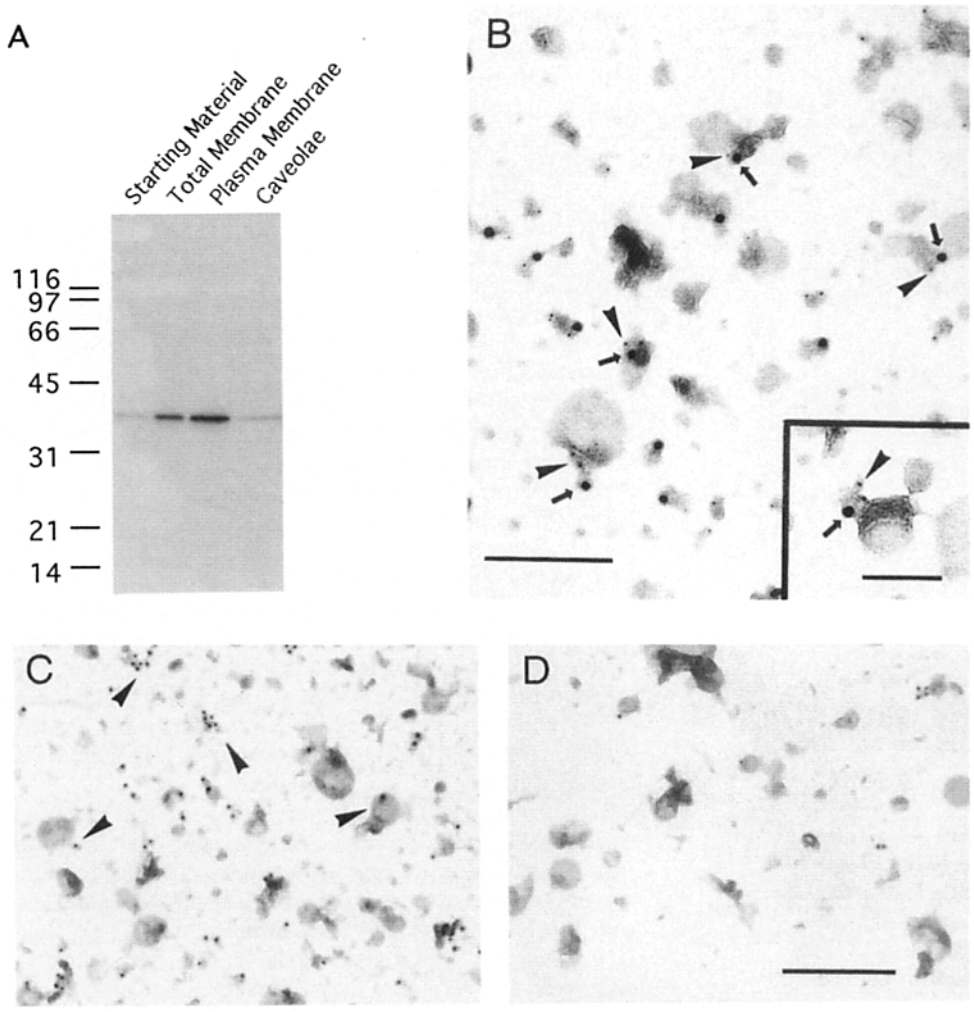

Figure 10. Immunoblot (*A*) and immunogold (*B*, *C*, and *D*) localization of G_β in fractions obtained during the purification of caveolae. (*A*) Samples (5 μg) of the indicated fraction were separated by electrophoresis on 11% polyacrylamide gels and immunoblotted with anti-G_β antisera (diluted 1:1,000) as described. Membrane III (*C*) or purified caveolae (*D*) were processed for whole mount immunogold labeling with anti-G_β antisera (diluted 1:1,000) as described in Fig. 9. Double labeling of Membrane III (*B*) was carried out by sequential addition of antibodies, using 5-nm gold for the anti-G_β antisera and 15-nm gold for the anti-caveolin IgG. Bar, 0.3 μm (*inset* bar, 0.1 μm).

There is now strong biochemical (5), morphological (40), and functional (6) evidence that it is the lipid environment of the caveolar membrane that attracts the fatty groups on the GPI-anchored proteins. Certain acylated cytoplasmic proteins may be attracted to caveolae for the same reason. Nonreceptor, tyrosine kinases have been found associated with caveolin-rich membranes (43) as well as clusters of GPI-anchored membrane proteins (7). Recently, Shenoy-Scaria et al. (45, Lublin, D. M., personal communication) showed that the interaction of $p56^{lck}$ and $p59^{fyn}$ with GPI-anchored protein complexes in Triton X-100 extracts depends on a thioester link to palmitate at position 3 in the amino-terminal sequence, Met-Gly-Cys. Myristoylation of the glycine is also required. All of the G_α subunits that we detected in purified caveolae share with $p59^{fyn}$ and $p56^{lck}$ the Met-Gly-Cys motif at the NH_2 terminus. Furthermore, all are palmitoylated at position 3 (9, 30, 33), and, with the exception of $G_{\alpha s}$, all have been found to be myristoylated at the Gly. These data suggest that the presence of two acylated amino acids in tandem may direct proteins to specialized membrane domains such as caveolae.

This model makes the prediction that the introduction of tandem acyl groups into a protein would direct it to caveolae/GPI anchor complexes. We found that $pp60^{c\ src}$ was not enriched in our purified caveolae preparations. However, $pp60^{c\ src}$ has the sequence Met-Gly-Ser and, therefore, can not be tandemly acylated. Lublin and co-workers (45, Lublin, D. M., personal communication) have now found that changing the Ser to a Cys causes both the tandem acylation of $pp60^{c\ src}$ and the association of the kinase with GPI anchor protein complexes. $G_{\alpha q}$ also appears to be enriched in caveolar preparations (43) but lacks the amino terminal myristoylation site (Gly). Instead, this protein has tandem cysteine residues at positions 9 and 10 that are both acylated (52). Therefore, tandem palmitoylation may work just as well to promote association with caveolae.

Acylation and deacylation of G_α appears to be a dynamic process (30). Acylation of one or more of the tandem sites may be the method the cell uses to control the location of the subunit on surface and internal membranes. This added level of cellular organization in the signaling cascade could ensure that G proteins are spatially positioned to optimize their interaction with the appropriate receptor/effector.

We also found evidence for the presence of small GTP-binding proteins in caveolae. [^{32}P]GTP blots showed that at least two proteins of 30 and 28 kD were enriched. Moreover, an anti-RaplA/B IgG was positive by both immunoblot and immunocytochemistry. RaplA/B shares extensive homology with ras protooncogenes (36) and can reverse the K-ras transformation of 3T3 cells (20). They also have been impli-

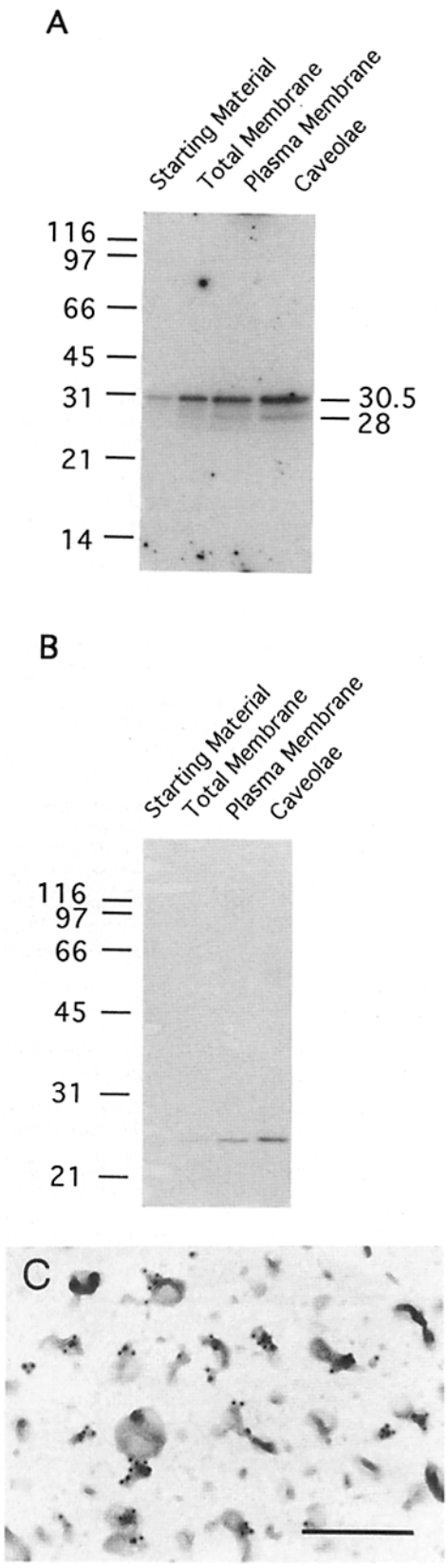

Figure 11. Radiolabeled GTP blot (*A*), immunoblot with anti-RaplA/B IgG (*B*), and immunogold localization of RaplA/B (*C*) in fractions obtained during the purification of caveolae. Samples (5 μg) of the indicated fraction were separated by electrophoresis on either 12.5% (*A*) or 11% (*B*) polyacrylamide gels and blotted with either ^{32}P-labeled GTP (*A*) or immunoblotted (*B*) with affinity purified polyclonal anti-peptide IgG against RaplA/B using alkaline phosphatase-labeled goat anti-rabbit IgG to detect the primary antibody. (*C*) The caveolae fraction was processed for whole mount immunogold labeling with anti-RaplA/B IgG as described. Bar, 0.3 μm.

cated in the negative regulation of ATP dependent Ca^{++} transport activity (8). Recent immunocytochemical studies have shown that Ca^{++} ATPase is present in caveolae (11). Therefore, the ras related Rapl GTP-binding protein may be involved in regulating cytosolic calcium fluxes through caveolae.

There are now two methods available for obtaining caveolae: the biochemical method we have developed and an analytical method described by Sargiacomo et al. (43). Our method has two main advantages. First, the availability of large quantities of caveolae will facilitate the identification of many of the protein and lipid components of the organelle. Second, Membrane III is quite enriched in caveolae so that it is possible to obtain quantities of the organelle without a detergent treatment step. This is important because of the finding that resident proteins like $G_{\beta\gamma}$ are removed by Triton X-100. Undoubtedly there are many important caveolae-associated molecules that will be removed using a purification scheme that depends on detergent. Nevertheless, the two types of preparations are in agreement that caveolae contain molecules that are known to participate in diverse signaling pathways. These isolation procedures set the stage for determining how caveolae function in the uptake of essential nutrients and in the delivery of signals to the cell.

This study would not have been possible without the dedicated assistance of Grace Liao who prepared the caveolae from chicken gizzards. We would like to thank Dr. Douglas Lublin for sharing his results before publication.

This work was supported by grants: HL 20948, GM 34497, and GM 43169 from the National Institutes of Health; BE30-0 from the American Cancer Society; 91R-077 from the American Heart Association; the Perot Foundation; The Lucille P. Markey Charitable Trust; and The Raymond Willie Chair of Molecular Neuropharmacology.

Received for publication 9 December 1993 and in revised form 11 March 1994.

References

1. Anderson R. G. W. 1993. Caveolae: where incoming and outgoing messengers meet. *Proc. Natl. Acad. Sci. USA.* In press.
2. Anderson, R. G. W. 1993. Potocytosis of small molecules and ions by caveolae. *TIC.* 3:69–71.
3. Anderson, R. G. W., B. A. Kamen, K. G. Rothberg, and S. W. Lacey. 1992. Potocytosis: sequestration and transport of small molecules by caveolae. *Science (Wash. DC).* 255:410–411.
4. Beranger, L., B. Goud, A. Tavitian, and J. de Gunzburg. 1991. Association of the Ras-antagonistic Rap1/Krev-1 proteins with the Golgi complex. *Proc. Natl. Acad. Sci. USA.* 88:1606–1610.
5. Cerneus, D. P., E. Ueffing, G. Posthuma, G. J. Strous, and A. van der Ende. 1993. Detergent insolubility of alkaline phosphatase during biosynthetic transport and endocytosis. Role of cholesterol. *J. Biol. Chem.* 268:3150–3155.
6. Chang, W.-J., K. G. Rothberg, B. A. Kamen, and R. G. W. Anderson. 1992. Lowering of the cholesterol content of MA104 cells inhibits receptor mediated transport of folate. *J. Cell Biol.* 118:63–69.
7. Cinek, T., and V. Horejsí. 1992. The nature of large noncovalent complexes containing glycosyl-phosphatidylinositol-anchored membrane glycoproteins and protein tyrosine kinases. *J. Immunol.* 149:2262–2270.
8. Corvazier, E., J. Enouf, B. Papp, J. D. Gunzburg, A. Tavitian, and S. Levy-Toledano. 1992. Evidence for a role of rap1 protein in the regulation of human platelet Ca2+ fluxes. *Biochem. J.* 281:325–331.

9. Degtyarev, M. Y., A. M. Spiegel, and T. L. Z. Jones. 1993. The G protein α_s subunit incorporates [^{3}H]Palmitic acid and mutation of cysteine-3 prevents this modification. *Biochemistry.* 32:8057–8061.
10. Dupree, P., R. G. Parton, G. Raposo, T. V. Kurzchalia, and K. Simons. 1993. Caveolae and sorting in the trans-Golgi network of epithelial cells. *Eur. Mol. Biol. Org. J.* 12:1597–1605.
11. Fujimoto, T. 1993. Calcium pump of the plasma membrane is localized in caveolae. *J. Cell Biol.* 120:1147–1157.
12. Fujimoto, T., S. Nakade, A. Miyawaki, K. Mikoshiba, and K. Ogawa. 1992. Localization of inositol 1,4,5-trisphosphate receptor-like protein in plasmalemmal caveolae. *J. Cell Biol.* 119:1507–1514.
13. Glenney, J. R. 1989. Tyrosine phosphorylation of a 22-kDa protein is correlated with transformation by Rous Sarcoma Virus. *J. Biol. Chem.* 264:20163–20166.
14. Glenney, J. R., and L. Zokas. 1989. Novel tyrosine kinase substrates from Rous Sarcoma Virus transformed cells are present in the membrane skeleton. *J. Cell Biol.* 108:2401–2408.
15. Hooper, N. M., S. J. Broomfield, and A. J. Turner. 1991. Characterization of antibodies to the glycosyl-phosphatidylinositol membrane anchors of mammalian proteins. *Biochem. J.* 273:301–306.
16. Hubbard, A. L., D. A. Wall, and A. Ma. 1983. Isolation of rat hepatocyte plasma membrane. I. Presence of the three major domains. *J. Cell Biol.* 96:217–229.
17. Kamen, B. A., C. A. Johnson, M. T. Wang, and R. G. W. Anderson. 1989. Regulation of the cytoplasmic accumulation of 5-methyltetrahydrofolate in MA104 cells is independent of folate receptor regulation. *J. Clin. Invest.* 84:1379–1386.
18. Kamen, B. A., A. K. Smith, and R. G. W. Anderson. 1991. The folate receptor works in tandem with a probenecid-sensitive anion carrier. *J. Clin. Invest.* 87:1442–1449.
19. Kamen, B. A., M. T. Wang, A. J. Streckfuss, X. Peryea, and R. G. W. Anderson. 1988. Delivery of folates to the cytoplasm of MA104 cells is mediated by a surface membrane receptor that recycles. *J. Biol. Chem.* 263:13602–13609.
20. Kitayama, H., Y. Sugimoto, T. Matsuzaki, Y. Ikawa, and M. Noda. 1989. A ras-related gene with transformation suppressor activity. *Cell.* 56:77–84.
21. Kurzchalia, T. V., P. Dupree, R. G. Parton, R. Kellner, H. Virta, M. Lehnert, and K. Simons. 1992. VIP21, a 21-kD membrane protein is an integral component of trans-Golgi-network-derived transport vesicles. *J. Cell Biol.* 118:1003–1014.
22. Lacey, S. W., J. M. Sanders, K. G. Rothberg, R. G. W. Anderson, and B. A. Kamen. 1989. cDNA for the folate binding protein correctly predicts anchoring to the membrane by glycosylphosphatidylinositol. *J. Clin. Invest.* 84:715–720.
23. Laemmli, U. K. 1970. Cleavage of structural proteins during the assembly of the head of bacteriophage T4. *Nature (Lond.).* 227:680–685.
24. Lapetina, E. G., and B. R. Reep. 1987. Specific binding of [α-^{32}P]GTP to cytosolic and membrane-bound proteins of human platelets correlates with the activation of phospholipase C. *Proc. Natl. Acad. Sci. USA.* 84:2261–2265.
25. Linder, M. E., P. Middleton, J. R. Hepler, R. Taussig, A. G. Gilman, and S. M. Mumby. 1993. Lipid modifications of G proteins: α subunits are palmitoylated. *Proc. Natl. Acad. Sci. USA.* 90:3675–3679.
26. Lisanti, M. P., M. Sargiacomo, L. Graeve, A. R. Saltiel, and E. Rodriguez-Boulan. 1988. Polarized apical distribution of glycosyl-phosphatidylinositol-anchored proteins in a renal epithelial cell line. *Proc. Natl. Acad. Sci. USA.* 85:9557–9561.
27. Lowry, O. H, N. J. Rosebrough, A. L. Farr, and R. J. Randall. 1951. Protein measurement with the folin phenol reagent. *J. Biol. Chem.* 193: 265–275.
28. Lucchesi, P. A., R. A. Cooney, C. Mangsen-Baker, T. W. Honeyman, and C. R. Scheid. 1988. Assessment of transport capacity of plasmalemmal Ca^{2+} pump in smooth muscle. *Am. J. Physiol.* 255:C226–C236.
29. Mumby, S. M., and A. G. Gilman. 1991. Synthetic peptide antisera with determined specificity for G protein α or β subunits. *Methods Enzymol.* 195:215–233.
30. Mumby, S. M., C. Kleuss, and A. G. Gilman. 1994. Palmitoylation of G protein α subunits: structural requirements and modulation by receptor agonist. *Proc. Natl. Acad. Sci. USA.* In press.
31. Deleted in proof.
32. Palade, G. E. 1953. Fine structure of blood capillaries. *J. Appl. Physics.* 24:1424.
33. Parenti, M., M. A. Viganó, C. M. H. Newman, G. Milligan, and A. I. Magee. 1993. A novel N-terminal motif for palmitoylation of G-protein α subunits. *Biochem. J.* 291:349–353.
34. Pathak, R. K., and R. G. W. Anderson. 1989. The use of dinitrophenol-IgG conjugates to detect sparse antigens by immunogold labeling. *J. Histochem. Cytochem.* 37:69–74.
35. Peters, K.-R., W. W. Carley, and G. E. Palade. 1985. Endothelial plasmalemmal vesicles have a characteristic striped bipolar surface structure. *J. Cell Biol.* 101:2233–2238.
36. Pizon, V., P. Chardin, I. Lerosey, B. Olofsson, and A. Tavitian. 1988. Human cDNAs rap1 and rap2 homologous to the Drosophila gene Dras3 encode proteins closely related to ras in the 'effector' region. *Oncogene.* 3:201–204.
37. Plourde, R., M. d'Alarcao, and A. R. Saltiel. 1992. Synthesis and characterization of an insulin-mimetic disaccharide. *J. Org. Chem.* 57: 2606-2610.
38. Romero, G., L. Luttrell, A. Rogol, K. Zeller, E. Hewlett, and J. Larner. 1988. Phosphatidylinositol-glycan anchors of membrane proteins: potential precursors of insulin mediators. *Science (Wash. DC).* 240:509–511.
39. Rothberg, K. G., J. E. Heuser, W. C. Donzell, Y.-S. Ying, J. R. Glenney, and R. G. W. Anderson. 1992. Caveolin, a protein component of caveolae membrane coats. *Cell.* 68:673–682.
40. Rothberg, K. G., Y.-S. Ying, B. A. Kamen, and R. G. W. Anderson. 1990. Cholesterol controls the clustering of the glycophospholipid-anchored membrane receptor 5-methyltetrahydrofolate. *J. Cell Biol.* 111: 2931–2938.
41. Rothberg, K. G., Y.-S. Ying, J. F. Kolhouse, B. A. Kamen, R. G. W. Anderson. 1990. The glycophospholipid-linked folate receptor internalizes folate without entering the clathrin-coated pit endocytic pathway. *J. Cell Biol.* 110:637–649.
42. Saltiel, A. R., and L. R. Sorbara-Cazan. 1987. Inositol glycan mimics the action of insulin on glucose utilization in rat adipocytes. *Biochem. Biophys. Res. Commun.* 149:1084–1092.
43. Sargiacomo, M., M. Sudol, Z. Tang, and M. P. Lisanti. 1993. Signal transducing molecules and GPI-linked proteins form a caveolin-rich insoluble complex in MDCK cells. *J. Cell Biol.* 122:789–808.
44. Shenoy, S. A., J. Kwong, T. Fujita, M. W. Olszowy, A. S. Shaw, and D. M. Lublin. 1992. Signal transduction through decay-accelerating factor: interaction of glycosyl-phosphatidylinositol anchor and protein tyrosine kinases p561ck and p59fyn. *J. Immunol.* 149:3535–3541.
45. Shenoy-Scaria, A. M., L. K. Timson Gauen, J. Kwong, A. S. Shaw, and D. M. Lublin. 1993. Palmitoylation of an amino-terminal cysteine motif of protein tyrosine kinases p561ck and p59fyn mediates interaction with glycosyl-phosphatidylinositol-anchored proteins. *Mol. Cell Biol.* 13: 6385–6392.
46. Simionescu, N., M. Simionescu, and G. E. Palade. 1972. Permeability of intestinal capillaries. *J. Cell Biol.* 53:365–392.
47. Simionescu, N., M. Simionescu, and G. E. Palade. 1975. Permeability of muscle capillaries to small heme-peptides: evidence for the existence of patent transendothelial channels. *J. Cell Biol.* 64:586–607.
48. Stefanová, I., V. Horejsí, I. J. Ansotegui, W. Knapp, and H. Stockinger. 1991. GPI-anchored cell-surface molecules complexed to protein tyrosine kinases. *Science (Wash. DC).* 254:1016–1019.
49. Sternweis, P. C., and J. D. Robinshaw. 1984. Isolation of two proteins with high affinity for guanine nucleotides from membranes of bovine brain. *J. Biol. Chem.* 259:13806–13813.
50. Thomas, P. M., and L. E. Samelson. 1992. The glycophosphatidylinositol-anchored Thy-1 molecule interacts with the p60fyn protein tyrosine kinase in T cells. *J. Biol. Chem.* 267:12317–12322.
51. Towbin, H., T. Staehelin, and J. Gordon. 1979. Electrophoretic transfer of proteins from polyacrylamide gels to nitrocellulose sheets: procedure and some applications. *Proc. Natl. Acad. Sci. USA.* 76:4350–4354.
52. Wedegaertner, P. B., D. H. Chutt, P. T. Wilson, M. J. Levis, and H. R. Bourne. 1993. Palmitoylation is required for signaling functions and membrane attachment of $G_q\alpha$ and $G_s\alpha$. *J. Biol. Chem.* 268:25001–25008.
53. Yamada, E. 1955. The fine structure of the gall bladder epithelium of the mouse. *J. Biophys. Biochem. Cytol.* 1:445–458.
54. Ying, Y.-S., R. G. W. Anderson, and K. G. Rothberg. 1992. Each caveola contains multiple glycosyl-phosphatidylinositol anchored membrane proteins. *Cold Spring Harbor Symp. Quant. Biol.* 57:593–604.